Quantitative prediction of twinning stress in fcc alloys: Application to Cu-Al

Sandeep A. Kibey,[1] L. L. Wang,[2] J. B. Liu,[2] H. T. Johnson,[1] H. Sehitoglu,[1] and D. D. Johnson[1,2,*]
[1]*Department of Mechanical Science and Engineering, University of Illinois, Urbana-Champaign, 1206 W. Green Street, Urbana, Illinois 61801, USA*
[2]*Department of Material Science and Engineering, University of Illinois, Urbana-Champaign, 1304 W. Green Street, Urbana, Illinois 61801, USA*

(Received 1 January 2009; revised manuscript received 4 May 2009; published 4 June 2009)

Twinning is one of most prevalent deformation mechanisms in materials. Having established a quantitative theory to predict onset twinning stress τ_{crit} in fcc elemental metals from their generalized planar-fault-energy (GPFE) surface, we exemplify its use in alloys where the Suzuki effect (i.e., solute energetically favors residing at and near planar faults) is operative; specifically, we apply it in Cu-xAl (x is 0, 5, and 8.3 at. %) in comparison with experimental data. We compute the GPFE via density-functional theory, and we predict the solute dependence of the GPFE and τ_{crit}, in agreement with measured values. We show that τ_{crit} correlates monotonically with the unstable twin fault energies (the barriers to twin nucleation) rather than the stable intrinsic stacking-fault energies typically suggested. We correlate the twinning behavior and electronic structure with changes in solute content and proximity to the fault planes through charge-density redistribution at the fault and changes to the layer- and site-resolved density of states, where increased bonding charge correlates with decrease in fault energies and τ_{crit}.

DOI: 10.1103/PhysRevB.79.214202 PACS number(s): 61.72.Bb, 61.72.Mm, 61.72.J−

I. INTRODUCTION

Twinning is a key deformation mechanism in low stacking-fault energy (SFE) bulk fcc alloys. Twin nucleation in fcc crystals is initiated by pre-existing dislocation configurations that dissociate into multilayered SF structures to nucleate a twin. Various qualitative criteria for twinning have been proposed that reflect the generalized planar fault-energy[1] (GPFE or γ) surface, such as so-called *twinability*[2–4] and those from simulations (arising from crack tips[5] and grain boundaries[6]) that are relevant to nanocrystalline metals. However, predicting the critical twinning stress τ_{crit} for twin nucleation in fcc alloys remains an outstanding problem.[7] Recently, we have linked τ_{crit} in elemental fcc metals to the twinning-energy pathways on the GPFE surface.[8] The theory contains also the directionality of twinning inherently through the GPFE (Ref. 9) for quantitative assessment of τ_{crit} in bulk systems. Here, we extend our theory to predict τ_{crit} in fcc alloys, where nucleation, electronic structure, defect energies, and the Suzuki effect[10,11] [solute attraction to (repulsion from) the defects] are all inextricably linked. Specifically, we consider Cu-xAl (x=0, 5, and 8.3 at. %) and we predict quantitatively the decreasing τ_{crit} (i.e., increased twinning propensity) due to addition of Al solute and correlate these with the decreasing unstable twin SFE, the barriers to twinning.[12] We also examine the effect of Al solute at and away from planar faults in Cu-xAl on the electronic charge-density distribution and density of states (DOS) and correlate it to lower fault energy and τ_{crit}.

Low SFE Cu-Al undergoes significant twinning during plastic flow.[13–17] In contrast to Cu, which does not twin except at high-strain rates and/or low (4 K) temperatures,[18] Cu-5% and 8%Al twin profusely at 77 and 300 K, respectively.[13,15] This increased twinning activity has been attributed to the lowering of intrinsic SFE (in mJ/m^2) γ_{isf} from 45 for Cu to 20 and 9 for 5% and 8% Al, respectively.[19,20] However, we have shown that the twinning in alloys strongly depends on their entire composition-dependent GPFE and not on γ_{isf} alone.[9,12]

As originally defined by Vitek,[1] the GPFE $\gamma(u_x)$ in fcc systems is the energy per unit area required to form m-layer faults by shearing m successive {111} layers along ⟨112⟩ through displacement u_x with γ_{us} as the stacking-fault nucleation barrier (or unstable intrinsic SFE), γ_{isf} as the one-layer intrinsic SFE, followed by the two-layer extrinsic unstable γ_{ue} and stable γ_{esf}, and then with γ_{ut} as the twin nucleation barrier (or unstable twin SFE), and $2\gamma_{tsf}$ as the twin boundary energy (or twice the twin SFE).[3–6,12,21] The γ surface dictates many effects such as dislocation motion,[22] nanoprecipitation in solid solutions,[23] and cross slip in $L1_2$ compounds.[24] Our previous results qualitatively showed that increased twinning tendency in Cu-xAl is primarily due to (i) a decrease in γ_{isf} and $2\gamma_{tsf}$ and (ii) a relatively larger decrease in twinning barrier γ_{ut}, which dominates a smaller decrease in γ_{us}.[9,12] However, for prediction and design purposes, it is essential to quantify the effect of the Al content on the twinning pathway GPFE and, hence, on τ_{crit} in alloys, which we do here for Cu-Al alloys.

II. CRITICAL TWINNING STRESS

Several dislocation-based models[25–28] have been proposed to explain twin nucleation in fcc materials. In many of these models, the critical (or onset) twinning stress τ_{crit} has been determined from the force required to operate a twin source, such as a dislocation pileup or Lomer-Cottrell locks.[26,27] Typically, these models require that τ_{crit} depends only on γ_{isf}—e.g., via a phenomenological relation $\tau_{crit}|\mathbf{b}_p| \sim K\gamma_{isf}$, with $\mathbf{b}_p$ as the Burgers vector for Shockley partials (i.e., $\mathbf{b}_p = a_0[11\bar{2}]/6$ in fcc elemental metals and solid solutions) and K as a fit parameter to ensure correlation with experimental data. However, twin nucleation in fcc crystals involves de-

TABLE I. Calculated (this study) bulk onset twinning stress for Cu-xAl τ_{crit}^{th} and ideal τ_{ideal}^{th} (in MPa) in agreement with experimental values τ_{crit}^{expt}. Cu-xAl fault energies (in mJ/m^2) are from Ref. 12. We also compare γ_{ut} for Cu at $N=3$ (nucleation) and $N>3$ (growth), $x=0$ s line. γ_{tsf} is ($N=3$) 15 versus ($N>3$) 11 mJ/m^2. Calculated Cu-Al γ_{isf} and $2\gamma_{tsf}$ are in agreement with experiment (in parentheses) but are not equal, as for pure elements, due to the Suzuki effect (Ref. 23).

x	γ_{us}	γ_{isf}	γ_{ue}	γ_{esf}	γ_{ut}	$2\gamma_{tsf}$	τ_{crit}^{th}	τ_{crit}^{expt}	τ_{ideal}^{th}
0	181	41	207	39	205	40	124	125–160[a]	3411
		(45)[b]			200	(48)[b]	120		
5	170	20	180	20	179	32	105	92–110[c]	3110
		(20)[b]				(34)[b]			
8.3	169	7	163	13	176	15	90	76–93[d]	3482
		(9)[b]							

[a]Reference 32.
[b]Reference 20 (0%, 5%, and 8% Al).
[c]Reference 14.
[d]Reference 17.

formation processes that span multiple length scales.

In our hierarchical approach for predicting τ_{crit} in fcc metals, Kibey *et al.*[8] accounted for deformation process associated with twinning at two different length scales: (a) at mesoscale level—where dislocations bounding the twin nucleus interact with each other—and (b) at atomic level—where lattice shears, due to passage of twinning partials, must traverse the twinning energy pathway given by GPFE. Our theory shows that the fcc twinning stress depends on the entire GPFE, shear modulus G on {111} planes, as well as the edge and screw components of the Burger's vector for shearing ($b_e^2=a_0^2/8$ and $b_s^2=a_0^2/24$, respectively), dislocations core width w ($0.2|\mathbf{b}_p|$ for fcc metals,[11] i.e., $a_0\sqrt{6}/30$), and geometry of the twin (width d and number of layers N in twin nucleus, i.e., three for fcc).[8] As a result, all parameters are quantities intrinsic to fcc materials, and there are no adjustable parameters in the equation for τ_{crit}. The twinning stress equation (in terms of $\tau(d)|\mathbf{b}_p|$ and extremal fault energies, so both are expressed in mJ/m^2) is given by

$$\begin{aligned}\tau(d)|\mathbf{b}_p| = {} & \frac{GN}{\pi d}\left[\frac{b_e^2}{4(1-\nu)}+\frac{b_s^2}{9}\right] \\ & + \frac{2}{3N}\left(\frac{3N}{4}-1\right)\left(\gamma_{ut}+\frac{(2\gamma_{tsf}+\gamma_{isf})}{2}\right) \\ & - \frac{2}{3N}(\gamma_{us}+\gamma_{isf}) + \frac{1}{6}\left(\gamma_{ut}-\frac{(2\gamma_{tsf}+\gamma_{isf})}{2}\right)\left(\frac{w}{d}\right) \\ & \times\left[\ln\left(\frac{d+\sqrt{d^2+w^2}}{w}\right)\right] \\ & + \left[\frac{1}{3N}(\gamma_{us}-\gamma_{isf}) - \frac{N-1}{3N}\left(\gamma_{ut}-\frac{(2\gamma_{tsf}+\gamma_{isf})}{2}\right)\right] \\ & \times\left(\frac{w}{d}\right)\left[\ln\left(\frac{d+\sqrt{d^2+w^2}}{w}\right)+\frac{d}{\sqrt{d^2+w^2}}\right]. \end{aligned} \quad (1)$$

The alloy shear modulus G (~17 GPa for Cu-xAl) was determined from the elastic moduli.[29–31] Thus, with the lattice constant a_0 known for each fcc system, only the twin width d is not known *a priori*. Hence, the $\tau(d)$ equation is minimized numerically subject to the constraint that $d \geq |\mathbf{b}_p|$, finding d and quantitatively determining the onset twinning stress τ_{crit}, as well as the aspect ratio of the twins.[8] The solutions of Eq. (1) were obtained for Cu-xAl using the GPFE data in Table I obtained in Ref. 12.

Equation (1) can be simplified, given that $N=3$ for a fcc twin nucleus, if (i) the width of a twin d is much larger than the width of a dislocation core w, i.e., $w/d \ll 1$,

$$\tau_{crit}|\mathbf{b}_p|\overbrace{N=3}\frac{5}{18}(\gamma_{ut}+2\gamma_{tsf})\left[1+\frac{1}{2}\frac{\gamma_{isf}-2\gamma_{tsf}}{\gamma_{ut}+2\gamma_{tsf}}\right] - \frac{4}{18}(\gamma_{us}+\gamma_{isf}). \quad (2)$$

Clearly, if the limits are valid, such that the twin aspect ratios are large, Eq. (2) is independent of G, w, and d—depending only on the extremal values of the GPFE. In this case, Eq. (2) yields 95–100 % of the τ_{crit} values in Table I, and, as such, it can be used for rapid assessments. A further simplification of Eq. (2) is possible if (ii) $\gamma_{isf}\sim 2\gamma_{tsf}\sim\gamma_{esf}$. However, while (ii) may be approximately correct for elemental metals (with central potentials[11]), as often quoted in the literature, it is not true for alloys,[23] as is evident for Cu-xAl (see Table I). So generally Eq. (2) must be used in its entirety, as detailed in what follows.

III. DETAILS OF CALCULATIONS

In order to determine (i) the stable and unstable defect energies for increasing layers of defects (i.e., GPFE or γ surface), (ii) the resulting onset twinning stress from Eq. (1) based on the density-functional-theory (DFT) calculated extremal values on the γ surface, and (iii) the electronic origin for reduction in γ_{isf} and onset stress τ_{crit} with addition of Al, we used density-functional theory based on plane-wave psueodpotential methods. Details of the density-functional-theory calculation (method, convergence studies, supercells, etc.) are given below and described elsewhere.[8,9,12,24,33] We used the Vienna *ab initio* Simulation Package[34] (VASP) within

the generalized gradient approximation[35] (GGA) and using the projector augmented wave[36] (PAW) basis for accuracy. We used periodic supercells consisting of M (111) fcc layers with four atoms per layer in the supercell (no free surfaces, ensuring bulk defects and simple convergence with respect to M). Translation vector $T_3=\mathbf{b}_p+M[111]$ maintained fcc symmetry across the periodic supercells, ensuring that no unfavorable A-A type stacking of (111) planes ever occurs. An intrinsic stacking fault was, for example, created by keeping the lower one to five layers fixed and sliding the remaining top layers along $[11\bar{2}]$ through one twinning partial $|\mathbf{b}_p|=a_0/\sqrt{6}$. For these cells, Brillouin-zone sampling was performed using $8\times8\times4$ special k-point mesh[37] with 273.2 eV energy cutoff, ensuring convergence of energy within ±1 meV/atom. Fault energies for Cu were converged when $M\geq9$. Full relaxation of atoms was allowed in the (111) fault layer and its adjacent (111) layers to yield a force below 3 meV/Å.

To remove the nonsystematic error associated with the DFT errors in the lattice constants to reveal correct trends for numerous systems, as noted before,[8,9,12] experimental lattice constants a_0^{expt} can be used to establish the periodicity of the supercells. As such correct trends are found among all systems, i.e., the separation between (111) planes is those found experimentally and the GPFE is more accurately determined. (A similar effect is well known, say, for the bulk modulus, where the curvature of the energy versus volume curve is in fact well described by DFT—so if you evaluate at a_0^{expt}, the bulk modulus agrees very well with the experiment, whereas the error in a_0^{DFT} leads to large error in bulk modulus.)

For Cu-5%Al (Cu-8.3%Al), to achieve the closest Al content near the samples addressed in experiment (5 and 8 at. % Al), we used a supercell with ten (nine) layers containing 40 (36) atoms per cell with two (three) solute atoms, a similar M that achieved converged fault energies in Cu. To address issues relevant to the Suzuki effect,[10,11] we explored which layer in Cu is most energetically favored by Al (near or away from the fault). In our previous study,[12] we placed Al in Cu-5%Al within second and sixth layers to ensure that mirror (positional) symmetry was maintained in all n-layer twin configurations; below we discuss the small effect of changing the Al atom positions with loss of mirror symmetry, which allows us to make comparisons of charge densities versus increasing solute content. Generally, the Al solute prefers to be neighboring the fault, decreasing energy cost of forming the fault (see below).

IV. RESULTS

In Table I, we compare to the measured data of the τ_{crit} predicted from our analytic theory that uses DFT-based GPFE as input. The predicted stresses are in excellent agreement with measured data, with no adjustable parameters. From our DFT fault energies, which are in quantitative agreement with those measured[12] (see Table I), our theory quantitatively captures the observed reduction in τ_{crit} in Cu-xAl with increasing %Al if the Suzuki effect is included; namely, the solute's most favorable location relative to the planar faults must be found, where Al favors being at the fault planes in Cu-Al, to obtain the minimum fault energies. For Cu, addition of Al reduces τ_{crit} from 124 to 105 and 90 MPa for 5% and 8.3% Al, respectively. Figure 1 provides the GPFE versus shearing along $[11\bar{2}]$ (in units of $|\mathbf{b}_p|$) and reveals the convergence of the twin energy and the Suzuki effect, in which the solute is near the fault and lowers the twinning barrier and various stable fault energies, hence, lowering τ_{crit}. Clearly, the (un)stable fault energies are concentration dependent, some more so. Also, the twinning barrier is at the formation of the $N=3$ twin nucleus, which gives the observed τ_{crit} of 124 MPa (see Table I and Fig. 1), reducing to 120 MPa for twin growth.

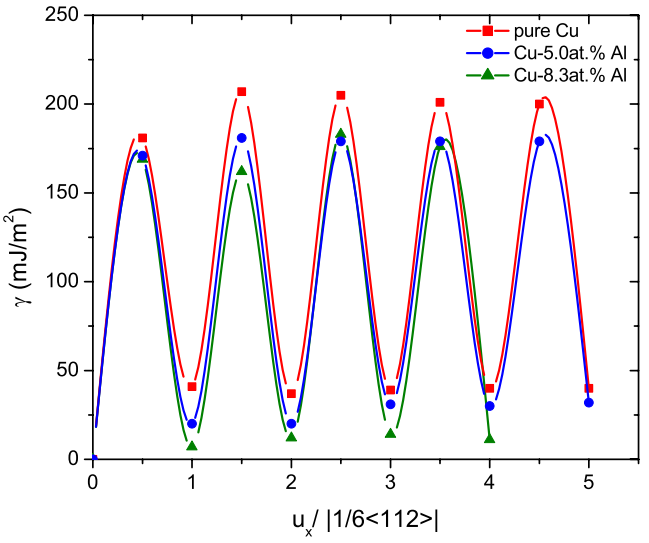

FIG. 1. (Color online) Planar defect energies (in mJ/m^2) versus displacement along $[11\bar{2}]$ (in units of $|\mathbf{b}_p|$) of layers above each successive fault plane, i.e., intrinsic SF (isf) at 1, extrinsic SF (esf) at 2, and twin fault (tsf) at 3, with additional layers extending the twin region. Unstable fault energies are at half units. After 5% Al γ_{ue} is smaller than γ_{ut}, which remains independent of concentration in the alloy.

Also in Table I is the oft-quoted "ideal" stresses, i.e., $\tau_{\text{ideal}}^{\text{th}}|\mathbf{b}_p|=\pi(\gamma_{\text{ut}}-2\gamma_{\text{tsf}})$, determined from an estimate of the derivative of the GPFE surface.[38] Clearly, because the ideal values do not incorporate the dislocation effects, they are ~30 times larger in magnitude than observed in fcc crystals. Moreover, the ideal stresses do not exhibit the observed monotonic decrease, as found experimentally and within our mesoscale dislocation theory.

For completeness, the trends from simple twinning measures, such as Berstein and Tadmor,[2,3] Van Swygenhoven *et al.*,[6] or Warner *et al.*,[5] can be directly assessed from our DFT-derived GPFE surface for elements[8] and alloys,[12] which we reported[12] previously for Cu-Al. We find that for elemental metals these measures do not predict the correct order; in Cu-Al, however, they do give the correct trend when alloying. The latter result can be attributed to the results shown in Figs. 1 and 2 and our observations are given next. Most importantly, our equation for τ_{crit} is equally simple as the above measures, provides a measurable quantity, and includes the asymmetry in stress for antitwinning.[9]

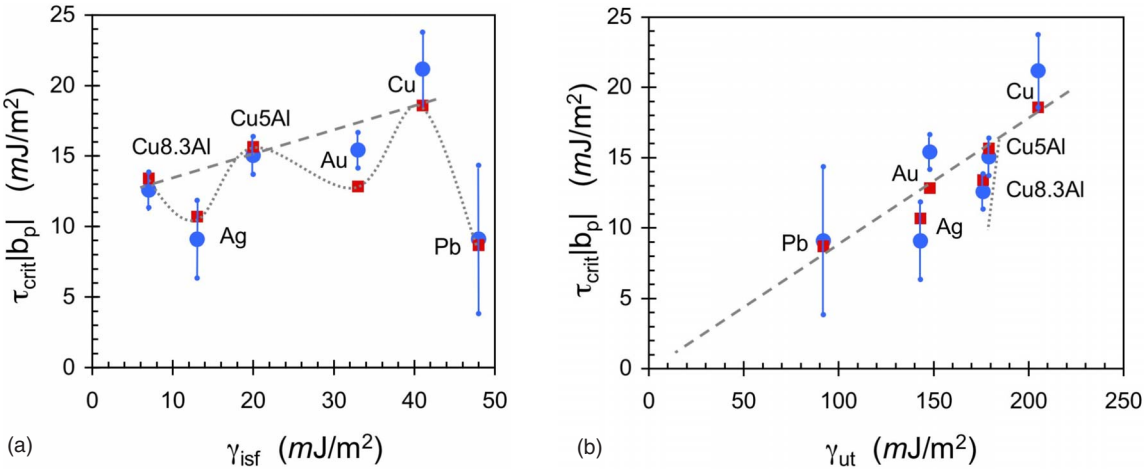

FIG. 2. (Color online) Predicted (squares) and experimental (circles) τ_{crit} for Cu-Al versus (a) γ_{isf} and (b) γ_{ut}, with comparison to other fcc metals from Ref. 8. Predicted τ_{crit} is in agreement with experimental data given by reported range of data (low, average, and high). Gray lines are guides for the eyes. In (a), τ_{crit} versus γ_{isf} exhibits *nonmonotonic* behavior (dotted gray line) contrary to that supposed in simple models. In contrast, in (b) there is a monotonic relation versus γ_{ut} (dashed gray line). In (a), within the Cu-Al, a monotonic relation versus γ_{isf} is apparent (dashed gray line) reflecting %Al-dependent drop of γ_{isf} (see Ref. 8), whereas in (b) there is a distinct change in τ_{crit} above 5% Al (dotted line), reflecting the more rapid drop in γ_{isf} (see text).

A. Twinning stress versus fault energies

In the past, while classical, phenomenological twinning-stress models[26,27] have proposed a monotonic (either linear or quadratic) relationship between τ_{crit} and γ_{isf} for all fcc materials. Figure 2 shows the τ_{crit} versus γ_{isf} and γ_{ut}, where the latter should be monotonic according to Eq. (1) or (2). Figure 2(a) clearly shows that monotonic dependence does not hold for fcc materials in general, i.e., elemental metals are not monotonic.[8] Also Cu-8.3%Al has lower SFE (7 mJ/m^2) than pure Ag does (18 mJ/m^2) but its twinning stress is higher (90 MPa) than that for Ag (65 MPa)—a result that cannot be explained through classical phenomenological models.

To understand this result, we examine the barriers involved in the twinning-energy pathway for these two fcc materials: the twinning nucleation barrier γ_{ut} for Cu-8.3%Al is much higher (176 mJ/m^2) than that for pure Ag (143 mJ/m^2; see Ref. 8), thus increasing the required shear stress to nucleate a twin. Figure 2(b) shows the variation in predicted and experimental twinning stress of fcc metals and alloys against γ_{ut}. The twinning stress for both fcc metals and alloys increases monotonically with twin nucleation barrier γ_{ut}, which indicates that γ_{ut} is an important material property controlling twin nucleation in both fcc metals and alloys. (For Ag, about a 5% change in γ_{ut} would have predicted result directly on the trend line also.) The apparent change in monotonic behavior after 5%Al for Cu-*x*Al system (dotted gray line in Fig. 2) arises due to composition dependence of SFE (see Fig. 1) and is observed experimentally (see Table I).

While τ_{crit} is not monotonic versus γ_{isf} for fcc elemental metals, contrary to what is often claimed, it is striking that the correlation appears to vary linearly for the Cu-*x*Al as a function of solute content. This monotonic behavior reflects the effect of alloying (the composition dependence) rather than universal behavior for twinning propensity related to the barriers controlling twin nucleation γ_{ut}, as we shall see when correlating the onset twinning stress to electronic density of states and charge densities.

Thus, we find that our theory for τ_{crit} holds for fcc metals as well as alloys and reveals a more general dependence of twinning stress on the entire GPFE and not on γ_{isf} alone. That τ_{crit} is nonmonotonic versus γ_{isf} for elemental metals and monotonic when alloying solute in a fixed solvent matrix is not evident from any previous studies but is found from the present theory, in agreement with experiment (see Fig. 2). Moreover, the present theory provides quantitative agreement with the observed twinning-stress values and quantitatively addresses the asymmetry in stress for antitwinning,[9] which provides correct assessment of twinning propensity in alloys.

B. Correlating to electronic effects

Previously, we have shown[12] that the increased twinning tendency within Cu-*x*Al (*x* is 5% and 8.3%) is primarily due to the dramatic decrease (by a factor of 3) in intrinsic SFE (see also Table I). In order to determine the electronic origin of the reduction in γ_{isf} (and twinning stress) due to Al addition, we examine the valence charge-density distribution and density of states for stacking faults in Cu-*x*Al. As with the defect energies, the charge densities and DOS were determined with VASP-PAW-GGA. The importance of the Suzuki effects is evident in the charge density and bonding.

1. Correlating to structure and charge distribution

As seen from the [111] stacking in Fig. 3(a) for 5% Al, one Cu atom was substituted by an Al within the second and fifth layers. For Cu-8.3%Al, in addition to the Al atoms in the second and fifth layers, an extra Al atom is substituted for a Cu atom within the eighth layer. As a result, the positions of the lower two Al atoms in Cu-5%Al and 8.3%Al are iden-

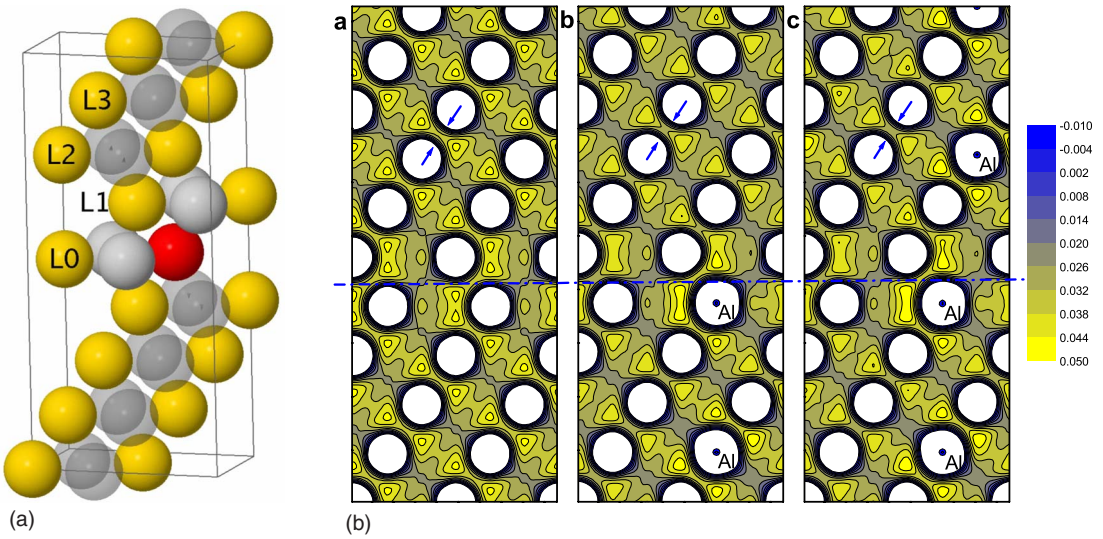

FIG. 3. (Color online) (a) Local structure and (b) valence-bonding charge density for an intrinsic SF in (i) Cu, (ii) Cu-5%Al, and (iii) Cu-8.3%Al. In (a), Al are shaded *red*, Cu in $[\bar{1}10]$ solute plane are *gold*, and out of plane are *gray*. (In grayscale, atoms are black, gray, and overlapping light gray, respectively). Dashed line marks the (111) SF plane just above the solute and the $[11\bar{2}]$ direction. Away from fault arrows mark comparable Cu-Cu bonds and the depletion of charge in Cu-Al (relative to pure Cu) due to substitutional Al. At fault plane, the Al enhances the charge for near-neighbor Cu, decreasing bonding, as shown by accumulation between out-of-plane Cu near Al.

tical (see stacking along [111] in Fig. 3(b)). Previously,[12] we placed Al in Cu-5%Al within second and sixth layers to ensure that mirror (positional) symmetry was maintained in all n-layer twin configurations. Here, changing the Al atom positions in Cu-5%Al to the second and fifth layers led to a small decrease in its γ_{isf} from 20 to 18.7 $\mathrm{mJ/m^2}$. However, keeping (a) the location of the fault identical in all supercells and (b) the lattice sites of first (lower) two Al atoms in Cu-xAl identical as well allowed us to compare the charge density in three fcc systems and identify the effect of Al on charge density.

The VASP-PAW-GGA-calculated bonding charge density of intrinsic stacking-fault structures in Cu-xAl (x=0%, 5%, and 8.3%) is plotted in the $(1\bar{1}0)$ plane [see Fig. 3(b)]. The bonding charge density is the valence charge density in the solid.[39,40] As shown in Fig. 3(b), there is a progressive increase in the valence charge in the vicinity of Al atom at the fault with increase in Al content from 0% and 5% to 8.3%, showing that substitutional Al increases charge near the defect consistent with the Suzuki effect.[10,11] Second, in Cu-xAl, the substitutional Al depletes charge from the first nearest-neighbor Cu-Cu bonding relative to an identical bonding site in pure Cu [indicated by arrows in Fig. 3(b)]. Both these effects increase from 0% to 8.3% Al, consistent with the decreasing γ_{isf} trend for Cu-xAl (see Table I). These Al-induced effects contribute in lowering the SFE in Cu-xAl making the γ_{isf} of Cu-8.3 at. %Al lowest of the three materials examined and, consequently, lead to a progressive reduction in twinning stress with increasing Al content. We expect similar charge-density distribution trends in Cu-Al with higher Al (11–14 at. %) content, also reported to twin profusely.[13,15] The same effects would be observed at a twin stacking fault, which gives the lowering of γ_{tsf}, as well as the unstable barriers, as we show here for intrinsic stacking fault.

2. Correlating the density of states and Suzuki effect

Besides changes in bonding charge, it is interesting to correlate the decrease in fault energies to the electronic DOS associated with the particular s, p, and d bonds and how the states are lowered in energy. In Fig. 4(a), we show the total DOS per atom for an intrinsic SF in Cu-xAl. In Fig. 4(b), we show the [111]-layer-specific Cu atom DOS for an intrinsic SF in Cu-xAl, which uses the layer notation given in Fig. 3(a).

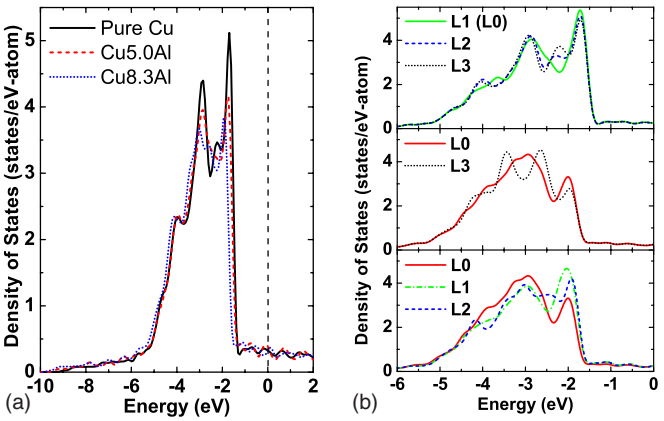

FIG. 4. (Color online) For Cu-xAl (a) total DOS per atom and (b) Cu atom DOS in a specific layer for an intrinsic SF. Energy zero is the Fermi energy. In (b), layer-specific Cu site DOS [L0 is below SF, L1 above SF, etc.; see Fig. 3(a)], with panels displaying Cu (top) and Cu-8.3%Al (middle and bottom). For Cu-8.3%Al results (middle and bottom), Al is in L0 (at the fault) and L3 (not at the fault) permitting determination of solute versus solute-fault effects. The Cu in L1 (L2) is at the fault (not at the fault) and has no intralayer solute. See text for discussion and details.

In Fig. 4(a), the total DOS shifts roughly and linearly with %Al after ~5% Al. This alloying effect reflects that solute begins to occur, on average, every three layers at ~5.5% Al, as can be verified in Fig. 3(b). (Other than this, the DOS does not reveal much of the details that are occurring due to alloying.) As a result, as shown in Fig. 2, τ_{crit} varies approximately linear versus γ_{isf} for Cu-xAl as a function of solute content. (Note, again, that τ_{crit} is not monotonic versus γ_{isf} for fcc elemental metals.) Thus, the monotonic behavior within a fixed system like Cu-xAl does not reflect universal behavior for twinning propensity related to the barriers controlling twin nucleation γ_{ut}, as already noted.

More revealing is the layer- and site-specific Cu DOS. In Fig. 4(b), we provide the Cu atom DOS in a particular layer, near or removed from solute and near or removed from the fault plane. The purpose is to discern whether it is just the solute affecting the lower of the planar-fault energies or rather it is the solute only in the vicinity of the planar fault that is the key for the dramatic lowering of the fault energies (which is the origin of the Suzuki phenomenon). Using Fig. 3(a) for reference, we see that L0 is below SF, L1 above SF, etc., and this is coordinated with the resolved Cu DOS in Fig. 4(b), where the top panel displaying pure Cu and the middle and bottom panels referring to Cu-8.3%Al. Without solute (top panel), the DOSs for Cu atoms in L0 and L1, both adjacent to fault, are equivalent, while L3 is equivalent to bulk. The effect of a SF on electronic structure that diminishes quickly as the Cu atom is further from the fault layer, due to electron screening, as seen by the similarity between the DOSs for Cu in L2 and L3. Clearly, compared to L2 and L3, the change in DOS of L1 (L0) at the SF is the appearance of a small pseudogap at −2.25 eV, where the peak (mostly composed of d_{xz} and d_{yz} characters) diminishes and is split into states above and below the former peak value. The change in DOS is due to the disruption in local stacking from fcc to hcp at the fault, altering mostly the d-band hybridization in d_{xz} and d_{yz}. The net effect is an increase in band energy or an energy increase to create an intrinsic SF in Cu. These results reveal the effects arising purely due to a fault.

Now we discuss the combined effect. For Cu-8.3%Al, an Al atom was introduced in L0 just below the fault plane, as shown in Figs. 3(a) and 3(b), as well as in L3 away from the fault, as shown in Fig. 3(b) (third panel). Figure 4(b) (middle panel) shows the Cu DOS adjacent to Al in L0 (at the SF) compared to L3 (not at the SF), hence, both Cu atoms have an intralayer interaction with Al. In contrast to L3, the Cu DOS in L0 still show the signature of the fault. As evident, a fault shifts states lower in energy compared to solute-only case (with more states around −3 eV), thereby reducing the SF energy. Figure 4(b) (bottom panel) shows the Cu atom DOS in L1 (at SF, no solute) and L2 (not at SF, no solute) compared to L0 (at SF, adjacent to solute). Clearly, the solute at the SF reduces the peak in antibonding states at the upper edge and produces a concomitant increase in DOS in the middle of the d band around −3 eV, both of which can be seen as the reason for the stabilization effect of Al solute to Cu stacking fault. As a result charge adjacent to solute is enhanced in its interstices for Cu atoms adjacent to the solute and only in the vicinity of the fault; this depletes charge from the Cu-Cu bonds thereby reducing γ_{isf} and γ_{ut}, a manifestation of the Suzuki effect.

V. SUMMARY

In summary, we have extended our hierarchical mesoscale dislocation theory for critical or onset twinning stress τ_{crit} in fcc metals to that of fcc alloys. Our analytic expression for τ_{crit} depends only on GPFE, shear modulus G on {111} fcc planes, dislocations core width w, and geometry of the twin nucleus (width d and number of twin layers N, which is three for a twin nucleus). As a result, all parameters are quantities intrinsic to fcc materials, and there are no adjustable parameters in the twinning-stress equation. We also give an approximate expression for τ_{crit} that depends only on GPFE extrema, which, nonetheless, is reasonably accurate. We, therefore, establish a quantitative dependence of twinning stress in fcc Cu-xAl alloys on their twinning-energy pathways including directionality.[9] The theory predicts twinning stresses for Cu-xAl in quantitative agreement with experimental results (without requiring any empiricism) using the DFT-derived (un)stable fault energies, which are also in quantitative agreement with observations. The results reveal a monotonic dependence of τ_{crit} on the unstable twin energy γ_{ut} indicating that twinning stress in Cu-Al alloys is intimately controlled by the twin nucleation barrier γ_{ut}. We find the solute-mediated decrease in the unstable extrinsic energy γ_{ue} is more dramatic than for γ_{ut}. We link the reduction in fault energies (and hence the twinning stress) with Al content to bonding-charge redistribution and the changes in layer- and atom-resolved electronic density of states. These results also highlight the critical role of the Suzuki effect, where solute is attracted to a planar defect and lowers the defect energy, as also recently highlighted as the cause for rapid precipitation in Al-Ag alloys.[23] It is found that Al increases charge in its interstices for Cu atoms adjacent to the solute and only in the vicinity of the fault; this depletes charge from the Cu-Cu bonds thereby reducing the stacking-fault energy in Cu-Al alloys—a general result of the Suzuki effect.

ACKNOWLEDGMENTS

This research was supported by National Science Foundation mainly under Grants No. DMR-08-03270, No. DMR-03-12448, and No. DMR-07-05089 with support from The Material Computation Center under Grant No. DMR-03-25939. Support for L.L.W. was given by the Department of Energy under Grant No. DE-FG02-03ER15476 with additional support for J.B.L. and D.D.J. under Grant No. DE-FG02-03ER46026.

*duanej@illinois.edu

[1] V. Vitek, Philos. Mag. **18**, 773 (1968).
[2] N. Bernstein and E. B. Tadmor, Phys. Rev. B **69**, 094116 (2004).
[3] E. B. Tadmor and N. Bernstein, J. Mech. Phys. Solids **52**, 2507 (2004).
[4] D. J. Siegel, Appl. Phys. Lett. **87**, 121901 (2005).
[5] D. H. Warner, W. Curtin, and S. Qu, Nature Mater. **6**, 876 (2007).
[6] H. Van Swygenhoven, P. M. Derlet, and A. G. Frøseth, Nature Mater. **3**, 399 (2004).
[7] J. W. Christian and S. Mahajan, Prog. Mater. Sci. **39**, 1 (1995).
[8] S. Kibey, J.-B. Liu, D. D. Johnson, and H. Sehitoglu, Acta Mater. **55**, 6843 (2007).
[9] S. Kibey, J.-B. Liu, D. D. Johnson, and H. Sehitoglu, Appl. Phys. Lett. **91**, 181916 (2007).
[10] H. Suzuki, J. Phys. Soc. Jpn. **17**, 322 (1962).
[11] J. Hirth and J. Lothe, *Theory of Dislocations*, 2nd ed. (Wiley-Interscience, New York, 1982).
[12] S. Kibey, J.-B. Liu, D. D. Johnson, and H. Sehitoglu, Appl. Phys. Lett. **89**, 191911 (2006).
[13] T. Mori and H. Fujita, Acta Metall. **28**, 771 (1980).
[14] F. Tranchant, J. Vergnol, M. F. Denanot, and J. Grilhe, Scr. Metall. **21**, 269 (1987).
[15] M. S. Szczerba, Mater. Sci. Eng., A **234-236**, 1057 (1997).
[16] M. Niewczas and G. Saada, Philos. Mag. A **82**, 167 (2002).
[17] M. S. Szczerba, T. Bajor, and T. Tokarski, Philos. Mag. **84**, 481 (2004).
[18] T. H. Blewitt, R. R. Coltman, and J. K. Redman, J. Appl. Phys. **28**, 651 (1957).
[19] C. B. Carter and I. L. F. Ray, Philos. Mag. **35**, 189 (1977).
[20] L. E. Murr, *Interfacial Phenomena in Metals and Alloys* (Addison-Wesley, Reading, MA, 1975).
[21] R. J. Asaro and S. Suresh, Acta Mater. **53**, 3369 (2005).
[22] G. Lu, N. Kioussis, V. V. Bulatov, and E. Kaxiras, Phys. Rev. B **62**, 3099 (2000).
[23] D. Finkenstadt and D. D. Johnson, Phys. Rev. B **73**, 024101 (2006).
[24] J.-B. Liu, D. D. Johnson, and A. V. Smirnov, Acta Mater. **53**, 3601 (2005).
[25] J. B. Cohen and J. Weertman, Acta Metall. **11**, 996 (1963).
[26] J. A. Venables, in *Deformation Twinning*, edited by R. E. Reed-Hill, J. P. Hirth, and H. C. Rogers (Gordon and Breach, New York, 1964), pp. 77–115.
[27] S. N. N. Muira and J.-I. Takamura, Trans. Jpn. Inst. Met. **9**, S555 (1968).
[28] S. Mahajan and G. Y. Chin, Acta Metall. **21**, 1353 (1973).
[29] D. Roundy, C. R. Krenn, M. L. Cohen, and J. W. Morris, Jr., Phys. Rev. Lett. **82**, 2713 (1999).
[30] L. Cain and J. F. Thomas, Jr., Phys. Rev. B **4**, 4245 (1971).
[31] We note that $G(111)=\frac{3C_{44}(C_{11}-C_{12})}{4C_{44}+C_{11}+C_{12}}$.
[32] A. Yamamoto, N. Narita, J. Takamura, H. Sakamoto, and N. Matsuo, J. Jpn. Inst. Met. **47**, 903 (1983).
[33] S. Kibey, J.-B. Liu, M. J. Curtis, D. D. Johnson, and H. Sehitoglu, Acta Mater. **54**, 2991 (2006).
[34] G. Kresse and J. Furthmuller, Phys. Rev. B **54**, 11169 (1996).
[35] J. P. Perdew and Y. Wang, Phys. Rev. B **45**, 13244 (1992).
[36] G. Kresse and D. Joubert, Phys. Rev. B **59**, 1758 (1999).
[37] H. J. Monkhorst and J. D. Pack, Phys. Rev. B **13**, 5188 (1976).
[38] S. Ogata, J. Li, and S. Yip, Phys. Rev. B **71**, 224102 (2005).
[39] G. Lu, D. Orlikowski, I. Park, O. Politano, and E. Kaxiras, Phys. Rev. B **65**, 064102 (2002).
[40] S. Schweizer, C. Elsasser, K. Hummler, and M. Fahnle, Phys. Rev. B **46**, 14270 (1992).